

A stochastic model for tumour control probability that accounts for repair from sublethal damage

ANA VICTORIA PONCE BOBADILLA^{†,‡}

*Wolfson Centre for Mathematical Biology, Mathematical Institute, University of Oxford,
Oxford OX2 6GG, UK*

[†]Corresponding author. Email: a.ponce@stud.uni-heidelberg.de

PHILIP K. MAINI AND HELEN BYRNE

*Wolfson Centre for Mathematical Biology, Mathematical Institute, University of Oxford,
Oxford OX2 6GG, UK*

[Received on 24 July 2016; revised on 12 December 2016; accepted on 19 December 2016]

The tumour control probability (TCP) is the probability that a treatment regimen of radiation therapy (RT) eradicates all tumour cells in a given tissue. To decrease the toxic effects on healthy cells, RT is usually delivered over a period of weeks in a series of fractions. This allows tumour cells to repair sublethal damage (RSD) caused by radiation. In this article, we introduce a stochastic model for tumour response to radiotherapy which accounts for the effects of RSD. The tumour is subdivided into two cell types: ‘affected’ cells which have been damaged by RT and ‘unaffected’ cells which have not. The model is formulated as a birth-death process for which we can derive an explicit formula for the TCP. We apply our model to prostate cancer, and find that the radiosensitivity parameters and the probability of sublethal damage during radiation are the parameters to which the TCP predictions are most sensitive. We compare our TCP predictions to those given by Zaider and Minerbo’s one-class model (Zaider & Minerbo, 2000) and Dawson and Hillen’s two-class model (Dawson & Hillen, 2006) and find that for low doses of radiation, our model predicts a lower TCP. Finally, we find that when the probability of sublethal damage during radiation is large, the mean field assumption overestimates the TCP.

Keywords: tumour control probability; radiation treatment of cancer; sublethal damage; mathematical modelling of cancer treatment.

1. Introduction

According to the World Health Organization, cancer is one of the leading causes of death worldwide, particularly in developing countries. For instance, in 2012, there were approximately 14 million new cases and over 8.2 million cancer related deaths (Stewart & Wild, 2014). Scientists have developed several treatments to fight this disease, the most common being surgery, chemotherapy and radiotherapy (RT) (Deisboeck *et al.*, 2011) with approximately 50% of all cancer patients receiving RT (Baskar *et al.*, 2012). In this article, we will be concerned with ionizing radiation (commonly x-rays) that aims to destroy the tumour mass while sparing the adjacent healthy tissue.

Radiation damages tumour cells mainly by inducing lesions in the DNA (Dale *et al.*, 2007). Lesions can be either single or double strand breaks. Double strand breaks are caused by a single

[†]Present address: Institute of Applied Mathematics, University of Heidelberg, Heidelberg 69120, Germany

event that targets both DNA strands, or by two independent single strand breaks in which the second one occurs, before the first break is repaired, in the same DNA locus (Halperin *et al.*, 2013). Double strand breaks cause lethal damage while single strand breaks can usually be repaired by the cell (Weinberg, 1983). In practice, several factors reduce the effectiveness of RT. These include: reoxygenation, redistribution, repopulation, radioresistance and RSD, which are known collectively as ‘the 5 Rs of radiobiology’ (Baskar *et al.*, 2014). In this work, we focus on RSD and its effect on treatment efficacy.

Fractionated treatments are widely used to deliver RT. Small doses of radiation are delivered to the affected region over a period of several weeks. The rationale for this treatment is that by giving smaller doses, toxic effects on healthy cells are reduced. However, since the dose is small, the cancer cells can repair themselves and one needs to take into account these repair mechanisms to accurately quantify the efficacy of the treatment (Pollack & Ahmed, 2011).

Mathematically, the objective of RT treatment planning can be stated as the establishment of a treatment protocol that maximizes the probability of cancer cell eradication and minimizes the probability of normal tissue complication. This gives rise to two key concepts: tumour control probability (TCP) and normal tissue complication probability (NTCP). TCP is the probability that a treatment regimen of RT eradicates all tumour cells in a given tissue, whereas NTCP estimates the negative side effects on the surrounding healthy tissue. These concepts are used to compare the expected success of different treatment protocols. In this work, we focus on TCP models, and ignore NTCP models but refer the reader to Baumann & Petersen (2004) and Stocks *et al.* (2016) for further details.

Most TCP models are based on the ‘linear quadratic’ (LQ) model. The LQ model is the most widely used model for studying the response of cells to RT (Lea *et al.*, 1962; Dale, 1996) and states that the survival fraction (SF) of the tumour mass after a single acute dose d Gy is given by

$$SF(d) = e^{-(\alpha d + \beta d^2)} \quad (1.1)$$

where α (Gy^{-1}) and β (Gy^{-2}) are tissue-specific radiosensitivity parameters (Brenner, 2008). The ratio α/β characterizes the radiosensitivity of tissues and can be used to classify tissues as either early ($\alpha/\beta \approx 10$) or late ($\alpha/\beta \approx 3$) responding tissues. Several extensions have been made to the LQ model to incorporate the 5 Rs of radiobiology (see Jones *et al.*, 2001; O’Rourke *et al.*, 2009 for a detailed development of the LQ formalism).

There are numerous mathematical models describing the effects of RT on tumour cells: continuous models (Enderling *et al.*, 2006; Ribba *et al.*, 2006; Rockne *et al.*, 2009; Bertuzzi *et al.*, 2010) and hybrid/discrete models (Enderling *et al.*, 2009; Richard *et al.*, 2009; Kempf *et al.*, 2010; Gao *et al.*, 2013; Powathil *et al.*, 2013): for a review see Enderling *et al.* (2010). In this work, we consider models where an explicit formula for the TCP can be obtained. The earliest and simplest expressions are based on Poisson and binomial distributions (Munro & Gilbert, 1961; O’Rourke *et al.*, 2009). By assuming the cell distribution after the radiation treatment follows a particular probability distribution, a statistical formula is obtained for the TCP. The Poisson TCP has been extensively used in clinical radiation treatment protocols and several extensions have been developed (O’Rourke *et al.*, 2009; Zaider & Hanin, 2011). The limitations of both the binomial and the Poisson TCP models are widely recognized (Tucker *et al.*, 1990; Yakovlev, 1993). In 2000, Zaider and Minerbo developed a non-Poissonian time-dependent TCP formula that could be applied to any treatment protocol (Zaider & Minerbo, 2000). They consider a stochastic birth–death process to include cellular repopulation. Several extensions to their formulation have been made to include cell cycle effects

(Dawson & Hillen, 2006; Hillen *et al.*, 2010; Dhawan *et al.*, 2014). Analysis of existing Poisson TCP models and birth–death process models have been presented by Hanin (2004) and Gong *et al.* (2011).

In this article, we introduce an extension of Zaider and Minerbo’s model that incorporates RSD. The outline of this article is as follows. In the next section, we introduce our model, we describe the mean dynamics and then the stochastic process that gives rise to it. We also derive an explicit formula for the TCP. In Section 3, we perform a parameter sensitivity analysis and find that variation in the radiosensitivity parameters and the probability of sublethal damage during radiation can significantly alter the TCP. We then compare our model with existing models, identifying conditions under which our model reduces to existing ones and others under which it yields different predictions. We observe that our model underestimates the TCP predicted by the Zaider and Minerbo (ZM) and Dawson and Hillen (DH) models for small radiation doses. We investigate when the mean field assumption cannot be justified and find that when the probability of sublethal damage is large this assumption is not valid. Lastly, in Section 4, we summarize and discuss our results.

2. Methods and model setup

Inspired by Zaider & Minerbo (2000), we develop a cell population model in the form of a continuous Markov chain model from which we can obtain an explicit expression for the TCP. First, we consider a deterministic cell population model that describes the mean dynamics of our stochastic model and accounts for cell proliferation and death, the effect of RT and the effect of sublethal damage.

To account for the different types of damage that RT can cause, we decompose the cancer cells into two classes: Unaffected (U) and Affected (A) cells. Let b_U, d_U, d_A and η be positive constants. Unaffected cells are assumed to proliferate and die at rates b_U and d_U , respectively. Affected cells do not proliferate but die at rate d_A . The death rates here correspond to programmed cell death independent of RT. Furthermore, we assume that affected cells recover from radiation damage at rate η .

We suppose that N doses of RT are delivered and denote by t_i the time at which the i -th treatment is administered. We assume that treatment is only delivered on week days and that it starts on a Monday. We assume the treatment acts instantaneously.

At treatment time t_i , we model lethal damage using the LQ model (Equation (1.1)). We assume different radiosensitivity parameters for the two classes. Let α_U, β_U and α_A, β_A be the radiosensitivity parameters of each class and SF_U, SF_A their respective survival fractions. The survival fraction of the unaffected class (SF_U) has the classic interpretation of the survival fraction: the fraction of clonogenic cells that survives a fractional dose (Hall *et al.*, 2006). For affected cells, which are by definition non-clonogenic, we assume that a fraction SF_A of them survives the fractionated dose and that it is smaller or equal to SF_U . We denote by $f(t_i^-)$ and $f(t_i^+)$ the values of the function $f(t)$ before and after the i -th treatment, respectively.

To include sublethal damage, we assume that the two cell classes respond differently at the treatment times. For the unaffected class, we assume three outcomes: (1) a proportion of the cells survives and is unaffected by RT, this factor is determined from the LQ model so that $U(t_i^+) = SF_U U(t_i^-)$; (2) a fraction, γ , of the cells harmed by RT acquire sublethal damage and switch to the affected class, $\gamma(1 - SF_U)U(t_i^-)$; (3) the remaining cells are eliminated due to lethal damage caused by radiation. We assume that the response of the affected cells to RT is simpler: the fraction of cells that survive is determined by the LQ model. Thus we suppose that $A(t_i^+)$, the number of cells in the affected class after treatment, is given by $A(t_i^+) = (SF_A)A(t_i^-) + \gamma(1 - SF_U)U(t_i^-)$. Finally, we assume that at the beginning of treatment we have N_0 cells in the unaffected class and none in the affected class. Under these assumptions, the deterministic

model can be written as follows:

$$\begin{cases} \frac{dU(t)}{dt} = (b_U - d_U)U(t) + \eta A(t), & t_i < t < t_{i+1}, \quad i = 0, 1, \dots, N, \\ \frac{dA(t)}{dt} = -(d_A + \eta)A(t), & t_i < t < t_{i+1}, \quad i = 0, 1, \dots, N, \\ U(t_i^+) = (SF_U)U(t_i^-), \quad A(t_i^+) = (SF_A)A(t_i^-) + \gamma(1 - SF_U)U(t_i^-), & \text{at } t = t_i, \quad i = 1, 2, \dots, N, \\ U(t_0) = N_0, \quad A(t_0) = 0. \end{cases} \tag{2.1}$$

We now can define a stochastic process whose mean behaviour is described by (2.1). We consider the evolution of the joint probability distribution, $p_{n_U, n_A}(t)$, which is the probability of having n_U and n_A cells in the unaffected and affected classes, respectively, at time t . As in the deterministic case, for the stochastic birth-death process we describe separately the evolution of the two cell types between treatment times and at treatment times.

Between treatment times t_i and t_{i+1} , the model follows a stochastic birth-death process, with constant birth (b_U) and death (d_U) rates for the unaffected class. We assume the affected class does not proliferate and follows a stochastic death process with death rate d_A and recovery rate η from A to U . The master equation associated with this process can be written as

$$\begin{aligned} \frac{d}{dt} p_{n_U, n_A}(t) = & -[(b_U + d_U)n_U + (d_A + \eta)n_A]p_{n_U, n_A}(t) + \eta(n_A + 1)p_{n_U - 1, n_A + 1}(t) \\ & + b_U(n_U - 1)p_{n_U - 1, n_A}(t) + d_U(n_U + 1)p_{n_U + 1, n_A}(t) + d_A(n_A + 1)p_{n_U, n_A + 1}(t) \end{aligned} \tag{2.2}$$

where $p_{-1, n_A}(t) = p_{n_U, -1}(t) = 0$ for $n_U, n_A \geq 0$.

We consider the initial conditions:

$$p_{n_U, n_A}(t_0) = 1, \quad \text{for } n_U = N_0 \text{ and } n_A = 0, \tag{2.3}$$

where N_0 is the initial number of cancer cells and $p_{n_U, n_A}(t_0) = 0$, for $(n_U, n_A) \neq (N_0, 0)$.

At each treatment time, the radiation response is modelled as a series of Bernoulli trials during which unaffected and affected cells survive with probabilities SF_U and SF_A , respectively. Sublethal damage is also modelled as a series of Bernoulli trials where an unaffected cell switches to the affected class with probability γ . From these Bernoulli series we derive the following expression for $p_{n_U, n_A}(t_i^+)$:

$$\begin{aligned} p_{n_U, n_A}(t_i^+) = & \sum_{j=0}^{\infty} P(n_U \text{ unaffected cells survived radiation}) \\ & \times P(j \text{ unaffected cells switched to the affected class}) \\ & \times P(n_A - j \text{ affected cells survived radiation}), \end{aligned}$$

which becomes

$$\begin{aligned} p_{n_U, n_A}(t_i^+) = & \sum_{k=0}^{\infty} \sum_{l=0}^{\infty} \sum_{j=0}^{n_A} p_{n_U + n_A - j + k, j + l}(t_i^-) \binom{j+l}{l} \binom{n_U + n_A - j + k}{n_U} \binom{n_A - j + k}{k} \\ & (SF_U)^{n_U} [\gamma(1 - SF_U)]^{n_A - j} (1 - \gamma(1 - SF_U) - SF_U)^k (SF_A)^j (1 - SF_A)^l. \end{aligned} \tag{2.4}$$

In summary, our model consists of the master equation (2.2), with the evolution at treatment time defined by Equation (2.4) and the initial conditions specified by Equation (2.3).

Finally, for this stochastic model, it is straightforward to show that the mean number of cells in each class, $\langle n_U(t) \rangle = \sum_{n_U=0}^{\infty} \sum_{n_A=0}^{\infty} n_U p_{n_U, n_A}(t)$ and $\langle n_A(t) \rangle = \sum_{n_U=0}^{\infty} \sum_{n_A=0}^{\infty} n_A p_{n_U, n_A}(t)$, satisfy Equation (2.1).

2.1 Derivation of the TCP

To obtain an explicit expression for the TCP, we consider the probability generating function (PGF) $G(t, x, y) = \sum_{n_U=0}^{\infty} \sum_{n_A=0}^{\infty} p_{n_U, n_A}(t) x^{n_U} y^{n_A}$. The evolution of the PGF satisfies a partial differential equation (PDE) that is derived from the master equation and the evolution of $p_{n_U, n_A}(t)$ at treatment times. Denoting by $G_i(t, x, y)$ the PGF during the interval $[t_i, t_{i+1}]$, it is possible to show that $G_i(t, x, y)$ evolves in the following way:

$$\begin{cases} \frac{\partial}{\partial t} G_i(t, x, y) = B_U(x) \frac{\partial}{\partial x} G_i(t, x, y) + D_A(x) \frac{\partial}{\partial y} G_i(t, x, y) & t_i < t < t_{i+1}, 0 < x, y < 1, \\ G_i(t_i, x, y) = G_{i-1}(t_i, F_U(x, y), G_A(y)) & 0 < x, y < 1, \\ G_0(t_0, x, y) = x^{N_0} & 0 < x, y < 1, \\ G_i(t, 0, 0) = p_{0,0}(t), G_i(t, 1, 1) = 1 & t_i < t < t_{i+1}, \end{cases} \tag{2.5}$$

where $B_U(x) = b_U x^2 - (b_U + d_U)x + d_U$, $D_A(x, y) = -(d_A + \eta)y + d_A + \eta x$, $F_U(x, y) = SF_U x + \gamma(1 - SF_U)y + 1 - \gamma(1 - SF_U) - SF_U$ and $G_A(y) = SF_A y + 1 - SF_A$.

The TCP at time t can be determined from the PGF, $G_i(t, x, y)$. We use the method of characteristics to solve the hyperbolic PDE for $G_i(t, x, y)$ and then obtain an explicit expression for the TCP:

$$TCP(t) := p_{0,0}(t) = G_i(t, 0, 0) \tag{2.6}$$

where

$$\begin{aligned} G_i(t, x, y) &= G_{i-1}(t_i, f_i(t, x, y), g_i(t, x, y)), \\ f_i(t, x, y) &= SF_U X(t - t_i, x) + \gamma(1 - SF_U)Y(t - t_i, x, y) + 1 - \gamma(1 - SF_U) - SF_U, \\ g_i(t, x, y) &= SF_A Y(t - t_i, x, y) + 1 - SF_A, \end{aligned}$$

in which

$$\begin{aligned} X(t, x) &= \frac{d_U(1-x)e^{(b_U-d_U)t} + b_U x + d_U}{b_U(1-x)e^{(b_U-d_U)t} + b_U x + d_U}, \\ Y(t, x, y) &= ye^{-(d_A+\eta)t} + \frac{d_A}{d_A + \eta} [1 - e^{-(d_A+\eta)t}] + \eta \int_0^t e^{-(d_A+\eta)t'} X(t', x) dt' \end{aligned}$$

and

$$G_0(t, x, y) = \left[\frac{(x-1)d_U e^{(b_U-d_U)t} - b_U x + d_U}{(x-1)b_U e^{(b_U-d_U)t} - b_U x + d_U} \right]^{N_0}. \tag{2.7}$$

X and Y are the characteristics of the hyperbolic PDE for $G_i(t, x, y)$ while f_i and g_i incorporate the effects of the stochastic evolution at the treatment times. A derivation of the TCP formula is included in Appendix A.

TABLE 1 Summary of parameter values used to simulate ZM (Equation (3.4)) DH (Equation (3.7)) and our model TCP (Equation (2.6)). The parameter values for the DH model are taken from Gong et al. (2011) while those for the ZM and our model are taken from Wang et al. (2003).

Description	TCP _{ZM}	TCP _{DH}	TCP _{RSD}	Units
Initial cell number	$N(0) = 10^5$	$a(0) = 10^5$ $q(0) = 0$	$U(0) = 10^5$ $A(0) = 0$	cells cells
Net growth rate	$b - d = 0.0165$	$\mu - d_a - d_q = 0.0165$	$b_U - d_U - d_A = 0.0165$	1/day
Kinetic parameters	$b = 0.0330$	$\mu = 0.1310$	$b_U = 0.1131$	1/day
	$d = 0.0165$	$d_a = 0.0655$	$d_U = 0.03$	1/day
		$v = 0.0476$	$\eta = 8.31$	1/day
		$d_q = 0.0952$		1/day
Radiosensitivity parameters	$\alpha = 0.14$	$\alpha_a = 0.145$	$\alpha_U = 0.14$	N/A* Gy^{-1}
		$\alpha_q = 0.145$	$\alpha_A = 0.14$	Gy^{-1}
	$\beta = 0.0452$	$\beta_a = 0.0353$	$\beta_A = 0.0452$	Gy^{-2}
		$\beta_q = 0.$	$\beta_Q = 0.0452$	Gy^{-2}

*Probability of unaffected cells to switch to the affected class

2.2 Case study: treatment of prostate cancer

In order to perform a parameter sensitivity analysis and model comparison we consider, as a case study, prostate cancer. Prostate cancer is a late responding, slow growing tumour. There is considerable uncertainty in its doubling time. For example, Wang et al. (2003) report doubling times in the range 15–170 days, with a median value of 42 days; this corresponds to a net growth rate of $0.0165 = \ln(2)/42$ per day. Based on this work and other reviews (Ritter, 2008), we estimate the range of doubling times to be 10–100 days while there are no direct methods available to measure *in vivo* apoptotic rates (Werahera et al., 2011), nevertheless the uncertainty in the apoptotic rates with a fixed net growth rate will turn out not to be significant for our model predictions. Following Wang et al. (2003), we suppose that the LQ parameters are within the following ranges $\alpha = 0.14 \pm 0.05 \text{ Gy}^{-1}$ and $\alpha/\beta = 3.1_{-1.6}^{+2.6} \text{ Gy}$. These ranges encompass all parameter ranges reported in the references mentioned above. The recovery rate for prostate cancer cells has been estimated to be 8.31 – 16.63 per day, although some authors report rates as high as 62.38 per day (Wang et al., 2003). In Table 1, we summarize the parameter values that we use to generate simulation results based on the previous biological studies.

3. Results

To investigate our model, we study the evolution of the TCP during treatment. Since the underlying model is stochastic, the TCP can be obtained as a statistic from multiple realizations of the stochastic process. For each realization i , we track the time t_i^* at which there are zero cancerous cells, and define $TCP_i(t)$ such that

$$TCP_i(t) := \begin{cases} 1 & t > t_i^*, \\ 0 & \text{otherwise.} \end{cases}$$

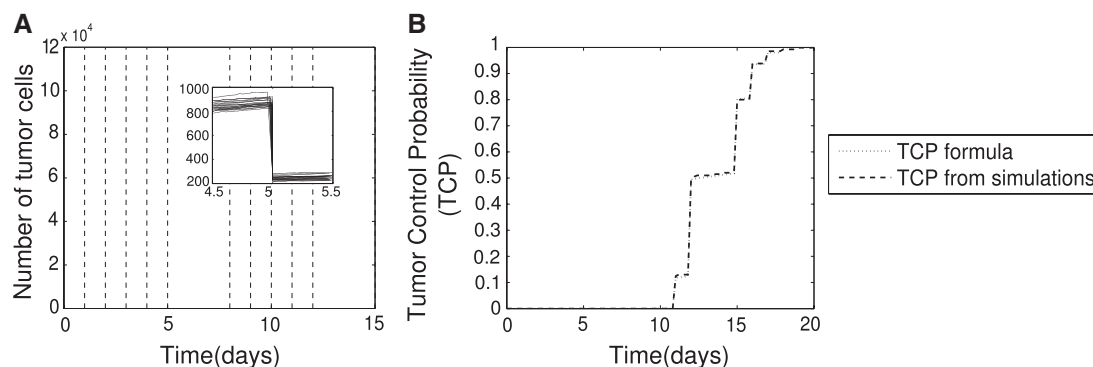


FIG. 1. (a) Time evolution of twenty realizations of the stochastic model (Equations (2.2)–(2.4)) generated using the Gillespie algorithm and the parameter values stated in Table 1. The treatment protocol consists of a dose per fraction of 4.3 Gy delivered on five consecutive days per week. The dashed lines indicate the times at which treatment is given (5 consecutive days per week). The inset highlights the variability between the realizations. (b) Plot of the approximation of the TCP (via Equation (3.1)) and of the TCP formula (Equation (2.6)).

After M simulations, the TCP is approximated by:

$$TCP(t) \approx \frac{1}{M} \sum_{i=1}^M TCP_i(t). \quad (3.1)$$

As the number of realizations increases, our approximation to the TCP for the stochastic process improves. However, as we have an explicit formula for the TCP for every time t (Equation (2.6)), we do not need to perform multiple realizations to calculate the TCP. In Fig. 1(a), we plot the output from 20 stochastic simulations, using the parameter values stated in Table 1. In the right corner of this figure, the magnification shows the different realizations and the associated stochasticity. From 500 such simulations, we approximate the TCP using Equation (3.1) and plot the resultant curve in Fig. 1(b). We also plot the TCP formula (Equation (2.6)) and observe good agreement between the two curves.

We continue below by presenting the results of a parameter sensitivity analysis. We then compare our model predictions with those of other models before finally analysing the validity of the mean field approximation.

Sensitivity analysis

The model parameters are either related to biological characteristics of the cancer (birth, death and recovery rates, radiosensitivity parameters and the probability of acquiring sublethal damage) or to the treatment protocol parameters (dose per fraction, number of fractions and total dose). Parameter values are obtained from clinical or experimental data, with confidence intervals (see Section 2.2). In what follows, we analyse the effects of varying the parameters in the reported ranges. Since our objective is to understand how RSD affects the TCP, we focus our sensitivity analysis on parameters associated with RSD: the repair rate, the radiosensitivity parameters for the two cell classes and the probability of an unaffected cell entering the affected class. When we vary a specific parameter, all other parameters are held fixed at the mean values reported in Table 1. Regarding the treatment protocol, we consider a dose per fraction of 4.3 Gy, delivered on five consecutive days per week: this is a standard protocol for

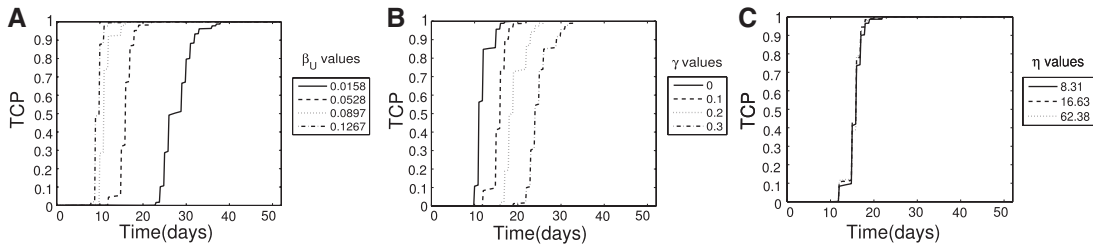


FIG. 2. Series of plots showing how the evolution of the TCP defined by Equation (2.6) changes as the parameters β_U , γ and η are varied. (a) Increasing β_U increases the rate at which the TCP approaches 1; (b) as γ increases, the time taken for the TCP to reach 1 also increases; (c) increasing η has negligible effect on the TCP dynamics. Parameter values as per Table 1. The treatment protocol consists of a dose per fraction of 4.3 Gy delivered on five consecutive days per week.

prostate cancer (Ritter, 2008). To improve the sensitivity analysis of the TCP curves, the simulations are continued beyond the treatment end time (16 days), until such time as all TCP curves reach the value 1.

First, we vary the radiosensitivity parameters in the ranges specified in Section 2.2. We assume both cell types have the same mean value for α and fix $\alpha_U = \alpha_A = 0.14$. We fix $\beta_A = 0.1267$ so the survival factor of the affected cells takes the smallest possible value. By varying β_U in the range $[0.0158, 0.1267]$ in steps of 0.037, we investigate how differences in the radiosensitivity of the two classes affects the TCP curve. The results presented in Fig. 2 (a) show that as β_U increases, the TCP reaches 1 more rapidly; this is to be expected, since higher values of β_U correspond to smaller survival fractions, so the tumour takes less time to disappear. If $\beta_U = 0.0158$, then $TCP(t) = 1$ for $t \geq 38$ days whereas if $\beta_U = 0.1267$, then $TCP(t) = 1$ for $t \geq 16$ days.

We now consider the impact on the TCP of varying γ , the proportion of cells that acquire sublethal damage in response to radiation (see Equation (2.1)). If $\gamma = 0$, then $A(t) = 0$ for $t \geq 0$ and all viable cells are unaffected. As γ increases, more unaffected cells acquire sublethal damage and the affected class plays a bigger role in the system dynamics. In Fig. 2 (b), we show how increasing γ increases the time taken for the TCP to reach 1, from 24 days when $\gamma = 0$ to 33 days when $\gamma = 0.3$. By contrast, varying η in the reported range has a negligible effect on the TCP (see Fig. 2(c)).

Comparison with other models

We now compare our TCP with those associated with the ZM and DH models.

In 2000, Zaider and Minerbo considered a homogeneous population of cells that undergoes a stochastic birth–death process with linear birth and death rates (Zaider & Minerbo, 2000). The master equation associated with this process can be written as

$$\frac{d}{dt}p_n(t) = b(n-1)p_{n-1}(t) + (d+h(t))(n+1)p_{n+1}(t) - (b+d+h(t))np_n(t), \quad (3.2)$$

where b and d are the birth and death rates, respectively. In Equation (3.2), the hazard function $h(t)$ models the effect of radiation on the cell population and depends on the radiosensitivity parameters α , β and the dose distribution $D(t)$ via

$$h(t) = (\alpha + 2\beta D(t)) \frac{dD(t)}{dt} = \frac{d}{dt}(\alpha D + \beta D^2). \quad (3.3)$$

From Equation (3.2), Zaider and Minerbo derived the following expression for the TCP:

$$TCP_{ZM}(t) = \left[1 - \frac{S_h(t)e^{(b-d)t}}{1 + bS_h(t)e^{(b-d)t} \int_0^t \frac{dr}{S_h(r)e^{(b-d)r}}} \right]^{n_0}, \tag{3.4}$$

wherein

$$S_h(t) = \exp\{-\alpha D(t) + \beta D^2(t) + \alpha D(0) + \beta D^2(0)\}.$$

Dawson and Hillen (2006) extended the ZM model to account for variation in radiosensitivity due to the cell cycle. They distinguish active ($a(t)$) and quiescent ($q(t)$) populations, with the following dynamics:

$$\begin{aligned} \frac{da}{dt} &= -\mu a + \nu q - (d_a + h_a(t))a, \\ \frac{dq}{dt} &= 2\mu a - \nu q - (d_q + h_q(t))q. \end{aligned} \tag{3.5}$$

Dawson and Hillen assumed that only active cells can proliferate and when an active cell divides, both daughter cells are quiescent. If μ denotes the proliferation rate, cell division leads to a loss term (μa) from the ordinary differential equation (ODE) for the active cells and a source term ($2\mu a$) in the ODE for the quiescent cells. Quiescent cells are assumed to re-enter the active compartment at rate $\nu > 0$.

In equations (3.5), $h_a(t)$ and $h_q(t)$ are the hazard functions, and d_a and d_q are the natural death rates of the active and quiescent cells, respectively. The hazard functions are derived from target theory principles considering one hit or two hit interactions

$$\begin{aligned} h_a(t) &= \alpha_a \frac{dD(t)}{dt} + \beta_a \frac{dD(t)}{dt} (D(t) - D(t - \omega)), \\ h_q(t) &= \alpha_q \frac{dD(t)}{dt} + \beta_q \frac{dD(t)}{dt} (D(t) - D(t - \omega)), \end{aligned} \tag{3.6}$$

where ω is the mean two-hit interaction time.

If the dose $D(t)$ is given in a time interval smaller than the mean two-hit interaction time, and additionally we have $\nu \ll 1$ and $\mu \ll 1$, then the hazard functions (3.6) reduce to (3.3) and we find that $\alpha = \min\{\alpha_a, \alpha_q\}$ and $\beta = \beta_a/2$ (Dawson & Hillen, 2006).

If $\nu \gg 1$, then $q \ll 1$ and $n = a + q \approx a$. In this case, addition of Equations (3.5) implies

$$\frac{da}{dt} = (\mu - d_a - h_a(t))a$$

and we recover the mean field dynamics of the ZM model.

TABLE 2 Treatment protocols to compare TCP predictions and references

Protocol	Dose/fraction (Gy)	Total days	Times/ day	Total dose (Gy)	Reference
A	2	52	once	78	Nilsson <i>et al.</i> (2004)
B	3.13	22	once	50	Ritter (2008)
C	4.3	16	once	51.6	Ritter (2008)

Dawson and Hillen (2006) reformulated their deterministic model (3.5) as a nonlinear birth–death process and, in so doing, derived the following expression for the TCP:

$$\begin{aligned}
 TCP_{DH} = & (1 - e^{-F(t)})^{q_0} (1 - e^{-G(t)})^{q_0} \exp \left[-v e^{-F(t)} \int_0^t q(z) e^{F(z)} dz \right. \\
 & \left. + \mu e^{-2G(t)} \int_0^t a(z) e^{2G(z)} dz - 2\mu e^{-G(t)} \int_0^t a(z) e^{G(z)} dz \right]
 \end{aligned} \tag{3.7}$$

where

$$F(t) = \int_0^t (\mu + h_a(z)) dz, \quad G(t) = \int_0^t (\mu + h_q(z)) dz,$$

and the functions $a(z)$ and $q(z)$ satisfy Equations (3.5) with $a(0) = a_0$ and $q(0) = q_0$.

Since the DM model deals with two cell populations, the master equation should be viewed as a differential equation for the joint probability of X_{n_a} and Y_{n_q} , the random variables that count the number of active and quiescent cells, respectively. We remark that in deriving Equation (3.7), Dawson and Hillen assumed the random variables X_{n_a} and Y_{n_q} to be independent.

To begin our model comparison, we first place our model in the same framework as these models. If the probability of moving from the unaffected to the affected class is zero ($\gamma = 0$), then we recover the ZM model. It is not possible to recover the DH model from our model, because the two classes in the DH model are based on the cell cycle whereas we distinguish damaged and undamaged cells, that is, each model accounts for different biological processes.

We compare the TCPs in a clinical setting by applying to each model the three treatment protocols for prostate cancer specified in Table 2. Protocol A is the standard one, while Protocols B and C are hypofractionated treatments which are specialized for slow growing tumours (higher doses per fraction are delivered over a shorter time period (Ritter, 2008)). We fix the net growth rate for the three models to 0.0165 and the hazard function as in Equation (3.3) for the ZM and DH models. In this setting, the discrepancies between the models' predictions are due to the biological processes implicit in each model. We compare the TCP for each model at the end of treatment since this quantity is used by clinicians to decide whether or not to apply treatment.

The TCPs for the three protocols are presented in Fig. 3. In each case, the DH and our model predict a smaller TCP than the ZM model; this is to be expected since both models consider two distinct cell populations (see also Gong *et al.* (2011)). In our model, the discrepancy arises because a proportion of irradiated cells are not killed and enter the affected class; in the DH model, the quiescent and active cells have different radiosensitivity parameters. For protocol A, at the end of the prescribed treatment ($t = 52$

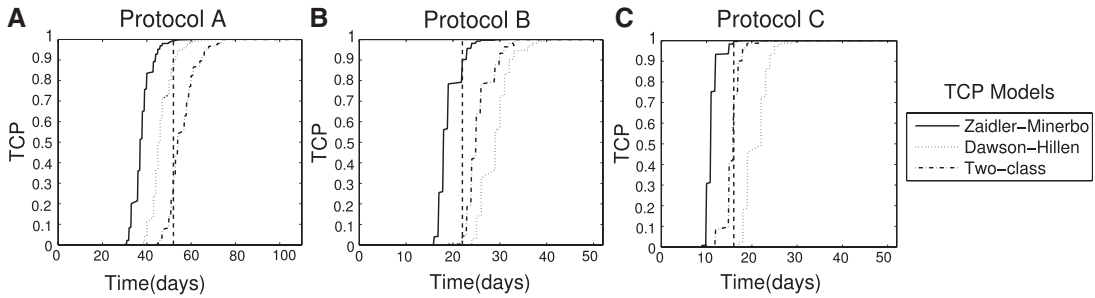


FIG. 3. TCP calculations for the protocols described in Table 2 for the ZM, DH and our two-class model (Equations (3.4), (3.7) and (2.6), respectively.) The calculations are performed using the parameter values listed in Table 1. In each subplot, the vertical dashed line marks the time at which the treatment ends. However, we continue the simulations beyond the treatment end point.

days), the ZM and DH models predict TCPs of 0.9946 and 0.8574, respectively, while our model predicts a TCP of 0.3273. For Protocol B, while the ZM model predicts a TCP of 0.9020, the other models predict $TCP < 0.05$. For Protocol C, at the end of treatment, the ZM model predicts a TCP of 0.999 while our model predicts a TCP of 0.7357. In this case, the DH model predicts no chance of tumour control. We remark that for these TCP calculations, we fixed $\gamma = 0.1$. However, our parameter sensitivity analysis indicates that if we increase γ then the TCP will be smaller (see Fig. 2(c)). We conclude that by suitable choice of γ our model will yield predictions similar to or lower than, those of the DH model. This highlights the importance of estimating γ from experimental data to obtain an accurate prediction.

Analysis of the mean field hypothesis

Existing models involving two cell populations (Dawson & Hillen, 2006; Hillen *et al.*, 2010) assume mean field dynamics to derive explicit formulae for the TCP. We now investigate, for our model, the range of parameter values for which this assumption is invalid.

First, we derive a TCP formula for our model by assuming mean field dynamics, so that $p_{n_U, n_A}(t) = p_{n_U}(t)p_{n_A}(t)$. We denote the TCP under this assumption as TCP_{mean} and write TCP_{real} for the TCP formula (2.6).

After some algebra (see Appendix B), we obtain the following expression for $TCP_{mean}(t)$:

$$TCP_{mean}(t) = v_i(t, 0)w_i(t, 0) \quad \text{for } t \in [t_i, t_{i+1}], \tag{3.8}$$

wherein

$$\begin{aligned} v_i(t, x) &= v_{i-1}(t_i, f_i(t, x))I_i(t, x), \\ w_i(t, x) &= v_{i-1}(t_i, 1 - \gamma(1 - SF)(1 - x)e^{-(d_A + \eta)(t-t_i)}) w_{i-1}(t_i, 1 - SF(1 - x)e^{-(d_A + \eta)(t-t_i)}), \\ n_i(t, x) &= 1 - \frac{SF(1 - x)(b_U - d_U)}{(b_U x - d_U)e^{-(b_U - d_U)(t-t_i)} + b_U(1 - x)}, \\ I_i(t, x) &= \exp \left[-\eta(1 - x)(b_U - d_U) \int_{t_i}^t \frac{A(s)e^{-(b_U - d_U)(s-t_i)} ds}{b_U(1 - x)e^{-(b_U - d_U)(s-t_i)} + (b_U x - d_U)e^{-(b_U - d_U)(t-t_i)}} \right], \end{aligned} \tag{3.9}$$

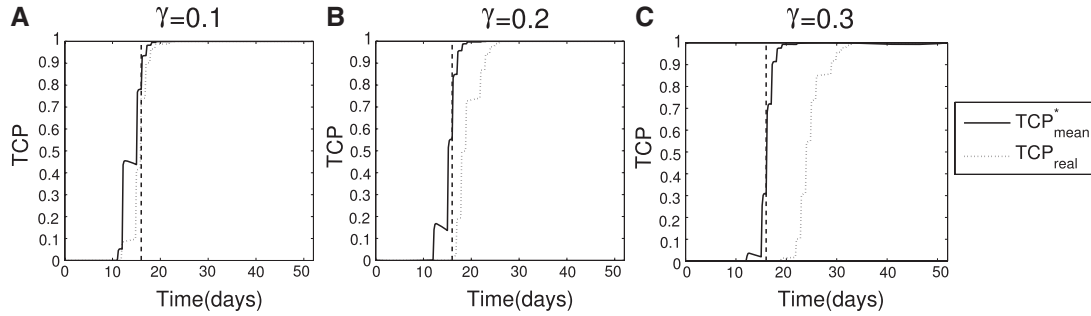


FIG. 4. Plots of discrepancy between the $TCP_{real}(t)$ as defined by Equation (2.6) and $TCP_{mean}^*(t)$ as defined by Equation (3.8) for $\gamma = 0.1, 0.2$ and 0.3 . The plots show that the difference between the TCP with the mean field dynamics assumption and the real TCP increases as γ increases. In each subplot, the vertical dashed line marks the time at which the treatment ends ($t = 16$ days). However, we continue the simulations beyond the treatment end point. Parameter values as per Table 1.

and $A(t)$ denotes the number of cells at time t , as defined by the mean dynamics (see Equations (2.1)). Finally, for $i = 0$, $v_0(t, x) = G_0(t, x)$ (Equation (2.7)) and $w_0(t, x) = 1$.

We consider the approximation to be valid when

$$\int_0^{T_{end}} |TCP_{real}(t) - TCP_{mean}^*(t)|^2 dt < TOL \quad (3.10)$$

where TOL is an acceptable deviation (TOL should be less than 0.10 (Brahme, 1984)).

We identify a range of parameters for which the inequality (3.10) is not satisfied. We focus in the case when the TCP calculated from the mean field assumption overestimates the true value, $TCP_{real}(t) \ll TCP_{mean}^*(t)$.

Given the difficulty of calculating $I_i(t, x)$ either explicitly or by discretization, in order to find a range of parameter values for which $TCP_{real}(t) \ll TCP_{mean}^*(t)$, we define a function $TCP_{mean}^*(t)$ such that $TCP_{mean}^*(t) < TCP_{mean}(t)$. We then find a range of parameter values for which $TCP_{real}(t) \ll TCP_{mean}^*(t)$. In this way, we can identify a range of parameter values for which inequality (3.10) does not hold. In Appendix C, we define $TCP_{mean}^*(t)$ and prove that $TCP_{mean}^*(t) < TCP_{mean}(t)$.

When identifying a parameter range for which inequality (3.10) does not hold, we note that as the value of γ is increased, the affected class plays a more significant role in the system dynamics. We anticipate that in such cases the mean field assumption will be less accurate. The results presented in Fig. 4 verify this. We consider Protocol C and three values for γ (0.1, 0.2 and 0.3). For each value of γ , $TCP_{real}(t) < TCP_{mean}^*(t)$; as the value of γ is increased, the discrepancy between the TCP predictions increases. We analyse how this difference affects the predicted TCP after 16 days of treatment with Protocol C. We present the computed TCP values after the 16 days for $\gamma = 0.1, 0.2$ and 0.3 in Table 3. We conclude that when $\gamma = 0.1$, the difference between the predictions is not significant whereas for larger values of γ it is.

4. Discussion

We have introduced a new TCP model that incorporates RSD. The model assumes the tumour is subdivided into two cell populations: affected cells which have sublethal damage and unaffected cells which have not. Between treatment times, unaffected cells are assumed to proliferate and die while the affected cells

TABLE 3 *TCP values after 16 days of treatment of $TCP_{real}(t)$ as defined by Equation (2.6) and $TCP_{mean}^*(t)$ as defined by Equation (3.8) for $\gamma = 0.1, 0.2$ and 0.3 . As the value of γ is increased, the discrepancy between the TCP predictions increases*

γ value	$TCP_{mean}^*(16)$	$TCP_{real}(16)$
0.1	0.78	0.73
0.2	0.55	0.02
0.3	0.30	0

do not proliferate but recover to the unaffected class and die at a certain rate. At treatment times, both classes are affected by radiation and the unaffected cells have the possibility of acquiring sublethal damage (move to the affected class) with a certain probability. The model is formulated as a birth–death process for which we derived an explicit formula for the TCP without making a mean field approximation, that is, by not assuming the random variables that count the cell number in each population are independent. We showed how changes in the model parameters affect the TCP predictions and how our model predictions compare to those of existing models in clinically relevant situations. Finally, we identified that when the probability of sublethal damage during radiation is large, the mean field assumption significantly overestimates the TCP.

Our model and Curtis’ lethal-potentially lethal (LPL) model both analyse irreparable and reparable lesions caused by RT, however, there are distinct assumptions and processes that one considers that the other does not. Our model takes into account cell repopulation whereas the LPL model assumes a stationary-phase cell population (Curtis, 1986). In the LPL model, potentially lethal lesions can transform to lethal ones throughout the treatment duration (Curtis, 1986), in our model, this is only possible at treatment times.

Our parameter sensitivity analysis revealed that increasing γ , the probability that an unaffected cell enters the affected class when RT is applied, significantly slows down the TCP. Given how sensitive the TCP is to variation in γ , we conclude that experimental estimates are needed in order to validate the model and/or to use it to make qualitative predictions. In future work, the parameter sensitivity analysis could be extended to determine whether changing the radiosensitivity parameters affects the TCP and to establish which parameters have the greatest impact on its dynamics.

We compared our model predictions with those of two existing models. As pointed out by Gong *et al.* (2011), since our model and the DH model consider two cell populations, the models predict lower TCPs than the ZM model. However, what we were interested in determining is how different our TCP predictions could be from the DH model, since Gong *et al.* (2011) claimed that TCP predictions from two cell population models are quite similar to each other. We found that for low radiation doses, our model yields TCPs which are significantly different from, and underestimate the TCP predicted by, the DH model. For high doses, the DH model underestimates our model predictions when $\gamma = 0.1$. However, for larger values of γ this trend reverses and our model underestimate the predictions from the DH model.

The way in which we formulate our model has several advantages. First, we can derive explicit expressions showing how the mean and variance of the cell number evolve during treatment. As a result, we can provide confidence intervals for the TCP predictions. Second, since we are working with an explicit TCP formula, minimal computational effort is needed to calculate the TCP. We emphasize that in contrast to existing TCP models that involve two cell populations, in our model, we did not make any

mean field dynamics assumptions. Additionally, we showed that for larger values of γ , the mean field dynamics are less accurate; they overestimate the TCP. In this work, we used an auxiliary function to identify the range of parameters for which the real value of the TCP and that obtained from the mean field assumption differ. In future work, it would be interesting to not use an auxiliary function and obtain the complete parameter range where this assumption is invalid.

Maler & Lutscher (2010) also formulated a cell population model without the independence assumption and compared it to the DH model. In order to incorporate realistic distributions of cell-cycle times, they formulated a deterministic age-structured model and a corresponding branching process. They showed that for fractionated treatments, their model underestimates the TCP in comparison to the DH model while for treatments that are constant in time, it gives similar predictions. They also analysed the effects of the compartmental independence assumption in the DH model. They found that by dropping the assumption of independence between active and quiescent cells, the TCP increases. This behaviour is contrary to what happens in our model: in their model not considering the independence assumption gives more conservative TCP predictions, while in ours, it overestimates the TCP.

In conclusion, we have introduced a new TCP model that includes RSD from which we were able to determine an explicit formula for the TCP. We identified the effects of parameter variation, we discovered clinically relevant situations when our model gives predictions which differ from those assumed with existing TCP models. We also identified parameter ranges for which the mean field assumption overestimates the TCP. There are several ways the model could be extended: we could account for the effects of hypoxia (Rockwell *et al.*, 2009), spatial heterogeneity (Enderling *et al.*, 2009) and angiogenic factors (Kleibeuker *et al.*, 2012) on treatment efficacy. Also, the current version of the model assumes RT is delivered instantly, whereas for certain treatment protocols the exposure to RT can last several days or even months (e.g. brachytherapy). Our model should be able to simulate these alternative dose distributions. Finally, while this work focused on prostate cancer, it could easily be extended to consider fast growing tumours, like head-neck or brain cancers (Fu *et al.*, 2000; Badri *et al.*, 2015).

Acknowledgements

The authors thank Dr Mike Partridge for useful discussions and AVPB wants to acknowledge the support of the Ecole Polytechnique Graduate School for allowing her to pursue this research project at the Wolfson Centre for Mathematical Biology, Mathematical Institute, Oxford.

Funding

Preparation of this work was supported by an Erasmus Mundus Scholarship provided to AVPB.

REFERENCES

- BADRI, H., PITTER, K., HOLLAND, E., MICHOR, F. & LEDER, K. (2015) Optimization of radiation dosing schedules for proneural glioblastoma. *J. Math. Biol.*, **72**, 1–36.
- BASKAR, R., DAI, J., WENLONG, N., YEO, R. & YEOH, K.-W. (2014) Biological response of cancer cells to radiation treatment. *Front. Biosci.*, **1**, 24.
- BASKAR, R., LEE, K. A., YEO, R. & YEOH, K.-W. (2012) Cancer and radiation therapy: current advances and future directions. *Int. J. Med. Sci.*, **9**, 193.
- BAUMANN, M. & PETERSEN, C. (2004) TCP and NTCP: a basic introduction. *Rays*, **30**, 99–104.
- BERTUZZI, A., BRUNI, C., FASANO, A., GANDOLFI, A., PAPA, F. & SINIGALLI, C. (2010) Response of tumor spheroids to radiation: modeling and parameter estimation. *Bull. Math. Biol.*, **72**, 1069–1091.

- BRAHME, A. (1984) Dosimetric precision requirements in radiation therapy. *Acta Radiol. Oncol.*, **23**, 379–391.
- BRENNER, D. J. (2008) The linear-quadratic model is an appropriate methodology for determining isoeffective doses at large doses per fraction. *Semin. Radiat. Oncol.*, **18**, 234–239.
- CURTIS, S. B. (1986) Lethal and potentially lethal lesions induced by radiation—a unified repair model *Radiat. Res.*, **106**, 252–270.
- DALE, R. (1996) Dose-rate effects in targeted radiotherapy. *Phys. Med. Biol.*, **41**, 1871.
- DALE, R. G., JONES, B. *et al.* (2007) *Radiobiological Modelling in Radiation Oncology*. London, UK: British Inst. of Radiology.
- DAWSON, A. & HILLEN, T. (2006) Derivation of the tumour control probability (TCP) from a cell cycle model. *Comput. Math. Methods Med.*, **7**, 121–141.
- DEISBOECK, T. S., WANG, Z., MACKLIN, P. & CRISTINI, V. (2011) Multiscale cancer modeling. *Annu. Rev. Biomed. Eng.*, **13**, 127–155.
- DHAWAN, A., KAVEH, K., KOHANDEL, M. & SIVALOGANATHAN, S. (2014) Stochastic model for tumor control probability: effects of cell cycle and (a) symmetric proliferation. *Theor. Biol. Med. Model.*, **11**, p. 1.
- ENDERLING, H., ANDERSON, A. R., CHAPLAIN, M. A., MUNRO, A. J. & VAIDYA, J. S. (2006) Mathematical modelling of radiotherapy strategies for early breast cancer. *J. Theor. Biol.*, **241**, 158–171.
- ENDERLING, H., CHAPLAIN, M. A. & HAHNFELDT, P. (2010) Quantitative modeling of tumor dynamics and radiotherapy. *Acta Biotheor.*, **58**, 341–353.
- ENDERLING, H., PARK, D., HLATKY, L. & HAHNFELDT, P. (2009) The importance of spatial distribution of stemness and proliferation state in determining tumor radioresponse. *Math. Model. Nat. Phenom.*, **4**, 117–133.
- FU, K. K., PAJAK, T. F., TROTTI, A., JONES, C. U., SPENCER, S. A., PHILLIPS, T. L., GARDEN, A. S., RIDGE, J. A., COOPER, J. S., ANG, K. K. *et al.* (2000) A radiation therapy oncology group (RTOG) phase III randomized study to compare hyperfractionation and two variants of accelerated fractionation to standard fractionation radiotherapy for head and neck squamous cell carcinomas: first report of RTOG 9003. *Int. J. Radiat. Oncol. Biol. Phys.*, **48**, 7–16.
- GAO, X., McDONALD, J. T., HLATKY, L. & ENDERLING, H. (2013) Acute and fractionated irradiation differentially modulate glioma stem cell division kinetics. *Cancer Res.*, **73**, 1481–1490.
- GONG, J., DOS SANTOS, M. M., FINLAY, C. & HILLEN, T. (2011) Are more complicated tumour control probability models better? *Math. Med. Biol.*, **30**, 1–19.
- HALL, E. J. & GIACCIA, A. J. (2006) *Radiobiology for the Radiologist*. Philadelphia, PA, USA: Lippincott Williams & Wilkins.
- HALPERIN, E. C., BRADY, L. W., WAZER, D. E. & PEREZ, C. A. (2013) *Perez & Brady's Principles and Practice of Radiation Oncology*. Philadelphia, PA, USA: Lippincott Williams & Wilkins.
- HANIN, L. G. (2004) A stochastic model of tumor response to fractionated radiation: limit theorems and rate of convergence. *Math. Biosci.*, **191**, 1–17.
- HILLEN, T., DE VRIES, G., GONG, J. & FINLAY, C. (2010) From cell population models to tumor control probability: including cell cycle effects. *Acta. Oncol.*, **49**, 1315–1323.
- JONES, L., HOBAN, P. & METCALFE, P. (2001) The use of the linear quadratic model in radiotherapy: a review. *Australas. Phys. Eng. Sci. Med.*, **24**, 132–146.
- KEMPF, H., BLEICHER, M. & MEYER-HERMANN, M. (2010) Spatio-temporal cell dynamics in tumour spheroid irradiation. *Eur. Phys. J. D.*, **60**, 177–193.
- KLEIBEUKER, E. A., GRIFFIOEN, A. W., VERHEUL, H. M., SLOTMAN, B. J. & THUISSEN, V. L. (2012) Combining angiogenesis inhibition and radiotherapy: a double-edged sword. *Drug Resist. Updat.*, **15**, 173–182.
- LEA, D. E. *et al.* (1962) Actions of radiations on living cells. *Actions of radiations on living cells*. London, UK: Cambridge University Press.
- MALER, A. & LUTSCHER, F. (2010) Cell-cycle times and the tumour control probability *Math. Med. Biol.*, **27**, 313–342.
- MUNRO, T. & GILBERT, C. (1961) The relation between tumour lethal doses and the radiosensitivity of tumour cells. *Br. J. Radiol.*, **34**, 246–251.
- NILSSON, S., NORLÉN, B. J. & WIDMARK, A. (2004) A systematic overview of radiation therapy effects in prostate cancer. *Acta Oncol.*, **43**, 316–381.

- O'ROURKE, S., MCANENEY, H. & HILLEN, T. (2009) Linear quadratic and tumour control probability modelling in external beam radiotherapy. *J. Math. Biol.*, **58**, 799–817.
- POLLACK, A. & AHMED, M. (2011) *Hypofractionation: Scientific Concepts and Clinical Experiences*. Ellicott City, MD, USA: LumiText Publishing.
- POWATHIL, G., ADAMSON, D. J. & CHAPLAIN, M. A. (2013) Towards predicting the response of a solid tumour to chemotherapy and radiotherapy treatments: clinical insights from a computational model. *PLoS Comput. Biol.*, **9**, e1003120.
- RIBBA, B., COLIN, T. & SCHNELL, S. (2006) A multiscale mathematical model of cancer, and its use in analyzing irradiation therapies. *Theor. Biol. Med. Model.*, **3**, 1.
- RICHARD, M., KIRKBY, K., WEBB, R. & KIRKBY, N. (2009) Cellular automaton model of cell response to targeted radiation. *Appl. Radiat. Isot.*, **67**, 443–446.
- RITTER, M. (2008) Rationale, conduct, and outcome using hypofractionated radiotherapy in prostate cancer. *Semin Radiat. Oncol.*, **18**, 249–256. Elsevier.
- ROCKNE, R., ALVORD JR, E., ROCKHILL, J. & SWANSON, K. (2009) A mathematical model for brain tumor response to radiation therapy. *J. Math. Biol.*, **58**, 561–578.
- ROCKWELL, S., DOBRUCKI, I. T., KIM, E. Y., MARRISON, S. T. & VU, V. T. (2009) Hypoxia and radiation therapy: past history, ongoing research, and future promise. *Curr. Mol. Med.*, **9**, 442–458.
- STEWART, B. & WILD, C. (2014) *World Cancer Report 2014*. Geneva, Switzerland: IARC Press, International Agency for Research on Cancer.
- STOCKS, T., HILLEN, T., GONG, J., & BURGER, M. (2016) A stochastic model for the Normal Tissue Complication Probability (NTCP) in radiation treatment of cancer. *Math. Med. Biol.*, **124**, 1–24.
- TUCKER, S. L., THAMES, H. D. & TAYLOR, J. M. (1990) How well is the probability of tumor cure after fractionated irradiation described by poisson statistics? *Radiat. Res.*, **124**, 273–282.
- WANG, J. Z., GUERRERO, M. & LI, X. A. (2003) How low is the α/β ratio for prostate cancer? *Int. J. Radiat. Oncol. Biol. Phys.*, **55**, 194–203.
- WEINBERG, R. A. (1983) A molecular basis of cancer. *Sci. Am.*, **249**, 126–142.
- WEAHERA, P. N., GLODE, L. M., LA ROSA, F. G., LUCIA, M. S., CRAWFORD, E. D., EASTERDAY, K., SULLIVAN, H. T., SIDHU, R. S., GENOVA, E. & HEDLUND, T. (2011) Proliferative tumor doubling times of prostatic carcinoma. *Prostate cancer*, **2011**, 1–7.
- YAKOVLEV, A. Y. (1993) Comments on the distribution of clonogens in irradiated tumors. *Radiat. Res.*, **134**, 117–120.
- ZAIDER, M. & HANIN, L. (2011) Tumor control probability in radiation treatment. *J. Med. Phys.*, **38**, 574–583.
- ZAIDER, M. & MINERBO, G. (2000) Tumour control probability: a formulation applicable to any temporal protocol of dose delivery. *Phys. Med. Biol.*, **45**, 279.

Appendix A. Derivation of the TCP formula

In this section, we derive the TCP formula (Equation (2.6)) for our stochastic model described by Equations (2.2) and (2.4).

Let

$$G_i(t, x, y) := \sum_{n_U=0}^{\infty} \sum_{n_A=0}^{\infty} x^{n_U} y^{n_A} p_{n_U, n_A}(t)$$

denote the PGF between treatment times $[t_i, t_{i+1}]$.

From the master equation (2.2), by multiplying by $x^{n_U} y^{n_A}$ and adding the terms from $n_U, n_A = 0$ to infinity, we obtain the hyperbolic equation for the PGF

$$\frac{\partial}{\partial t} G_i(t, x, y) = (b_U x^2 - (b_U + d_U)x + d_U) \frac{\partial}{\partial x} G_i(t, x, y) + [-(d_A + \eta)y + d_A + \eta x] \frac{\partial}{\partial y} G_i(t, x, y).$$

The initial condition for $G_0(t, x, y)$ is given by the initial condition of the deterministic model (Equation (2.1)) :

$$G_0(0, x, y) = \sum_{n_U=0}^{\infty} \sum_{n_A=0}^{\infty} p_{n_U, n_A}(0) x^{n_U} y^{n_A} = x^{N_0}.$$

The initial conditions for $G_i(t, x, y)$ with $i > 1$ are determined by the evolution of $p_{n_U, n_A}(t)$ at treatment times. We simplify expression (2.4) noticing that $p_{n,m}(t) = \frac{\partial^n}{\partial x^n} \frac{\partial^m}{\partial y^m} G(t, x, y)|_{(x,y)=(0,0)} = p_{n,m}(t)$ and identifying Taylor expansions in each variable, we deduce that

$$p_{n_U, n_A}(t_i^+) = \sum_{j=0}^{n_A} \frac{(SF_U)^{n_U} [\gamma(1 - SF_U)]^{n_A-j} (SF_A)^j}{j! n_U! (n_A - j)!} \frac{\partial^{(n_U+n_A-j)}}{\partial x^{(n_U+n_A-j)}} \frac{\partial^j}{\partial y^j} G(t_i, x, y) \Big|_{\substack{x=1-\gamma(1-SF_U)-SF_U \\ y=1-SF_A}}. \tag{A.1}$$

Substituting (A.1) in $G_i(t_i, x, y) = \sum_{n_U=0}^{\infty} \sum_{n_A=0}^{\infty} p_{n_U, n_A}(t_i^+, x, y)$ and noticing the resultant expression is a Taylor expansion in two variables enables us to derive the following expression which relates the PGFs before and after RT:

$$G_i(t_i, x, y) = G_{i-1}(t_i, SF_U x + \gamma(1 - SF_U)y + 1 - \gamma(1 - SF_U) - SF_U, SF_A y + 1 - SF_A).$$

In summary, $G_i(t, x, y)$ satisfies the following PDE:

$$\begin{cases} \frac{\partial}{\partial t} G_i(t, x, y) = B_U(x) \frac{\partial}{\partial x} G_i(t, x, y) + D_A(x, y) \frac{\partial}{\partial y} G_i(t, x, y) & t_i < t < t_{i+1}, \quad 0 < x, y < 1, \\ G_i(t_i, x, y) = G_{i-1}(t_i, F_U(x, y), G_A(y)) & 0 < x, y < 1, \\ G_0(t, x, y) = x^{N_0} & 0 < x, y < 1, \\ G_i(t, 0, 0) = p_{0,0}(t), \quad G_i(t, 1, 1) = 1 & t_i < t < t_{i+1}, \end{cases} \tag{A.2}$$

where $B_U(x) = b_U x^2 - (b_U + d_U)x + d_U$, $D_A(x, y) = -(d_A + \eta)y + d_A + \eta x$, $F_U(x, y) = SF_U x + \gamma(1 - SF_U)y + 1 - \gamma(1 - SF_U) - SF_U$ and $G_A(y) = SF_A y + 1 - SF_A$.

We use the method of characteristics to solve for $G_i(t, x, y)$. First we determine the characteristic curves $\mathbb{X}(t) = (X(t), Y(t))$,

$$\begin{cases} \frac{d}{dt} X(t) = -(b_U X^2 - (b_U + d_U)X + d_U), \\ \frac{d}{dt} Y(t) = -[-(d_A + \eta)Y + d_A + \eta X], \\ X(t_0) = x_0, Y(t_0) = y_0. \end{cases}$$

We have that

$$X(t) = \frac{d_U(1 - x_0)e^{(b_U-d_U)(t_0-t)} + b_U x_0 + d_U}{b_U(1 - x_0)e^{(b_U-d_U)(t_0-t)} + b_U x_0 + d_U}$$

and

$$Y(t) = y_0 e^{(d_A+\eta)(t-t_0)} + \frac{d_A}{d_A + \eta} [1 - e^{(d_A+\eta)(t-t_0)}] - \eta e^{(d_A+\eta)t} \int_{t_0}^t e^{-(d_A+\eta)t'} X(t') dt'. \tag{A.3}$$

Since the solution of (A.2) is constant along the characteristics it is sufficient to take the initial condition to determine the solution. At point (t_0, x_0, y_0) , the solution is given by $G_i(t_{i+1}, SF_U X(0) + \gamma(1 - SF_U)Y(0) + 1 - \gamma(1 - SF_U) - SF_U, SF_A Y(0) + 1 - SF_A)$ for $i > 1$ and $X(0)^{N_0}$ for $i = 0$. Since we want the solution for $(t - t_i, x, y)$, we make the change of variables: $x_0 \rightarrow x, y_0 \rightarrow y, t_0 \rightarrow t - t_i$. We have then that for $t \in [t_0, t_1]$,

$$G_0(t, x, y) = \left[\frac{(x - 1)de^{(b_U - d_U)t} - b_U x + d_U}{(x - 1)b_U e^{(b_U - d_U)t} - b_U x + d_U} \right]^{N_0} \tag{A.4}$$

and for $t \in [t_i, t_{i+1}]$ with $i > 1$

$$G_i(t, x, y) = G_{i-1}(t_i, f_i(t, x, y), g_i(t, x, y)) \tag{A.5}$$

where

$$\begin{aligned} f_i(t, x, y) &= SF_U X(t - t_i, x) + \gamma(1 - SF_U)Y(t - t_i, x, y) + 1 - \gamma(1 - SF_U) - SF_U, \\ g_i(t, x, y) &= SF_A Y(t - t_i, x, y) + 1 - SF_A, \\ X(t, x) &= \frac{d_U(1 - x)e^{(b_U - d_U)t} + b_U x + d_U}{b_U(1 - x)e^{(b_U - d_U)t} + b_U x + d_U} \end{aligned}$$

and

$$Y(t, x, y) = ye^{(d_A + \eta)(-t)} + \frac{d_A}{d_A + \eta} [1 - e^{-(d_A + \eta)t}] + \eta \int_0^t e^{-(d_A + \eta)t'} X(t') dt'.$$

Equation (A.5) defines a recursive formula for the PGF from which an explicit formula can be derived in terms of $G_0(t, x, y)$ and model parameters.

Appendix B. Derivation of the TCP formula under mean field dynamics

In this section, we derive the TCP formula (Equation (3.8)) for our stochastic model under the mean field assumption.

When we make the mean field approximation

$$p_{n_U, n_A}(t) = p_{n_U}(t)p_{n_A}(t), \tag{B.1}$$

we are assuming that the two cell populations are independent and have distinct PGFs. For $t \in [t_i, t_{i+1}]$, let $v_i(t, x) = \sum_{n_U=0}^{\infty} p_{n_U}(t)x^{n_U}$ and $w_i(t, x) = \sum_{n_A=0}^{\infty} p_{n_A}(t)x^{n_A}$ denote the PGFs for the unaffected and affected classes, respectively.

If we multiply the master equation (2.2) by x^{n_U} and sum the resulting equations from $n_U = 0$ to $n_U \rightarrow \infty$ then we obtain the following hyperbolic PDE for $v_i(t, x)$:

$$\frac{\partial v_i(t, x)}{\partial t} = [b_U x^2 - (b_U + d_U)x + d_U] \frac{\partial v_i(t, x)}{\partial x} + \eta(x - 1)A(t)v_i(t, x),$$

where $A(t) = \sum_{n_A=0}^{\infty} n_A p_{n_A}(t)$ denotes the mean number of active cells at time t and its dynamics is defined by Equation (2.1).

As for the derivation of the TCP formula in Appendix B, the initial condition for $v_i(t, x)$ with $i > 1$ is determined from the evolution of $p_{n_U}(t)$ at the treatment times via

$$v_i(t_i, x) = v_{i-1}(t_i, 1 + SF(x - 1)).$$

The boundary conditions are determined by noting that $v_i(t, x)$ is a PGF with

$$v_i(t, 0) = p_0(t), \quad \text{and} \quad v_i(t, 1) = 1.$$

In summary, $v_i(t, x)$ satisfies the following boundary value problem

$$\left\{ \begin{array}{ll} \frac{\partial v_i(t,x)}{\partial t} = [b_U x^2 - (b_U + d_U)x + d_U] \frac{\partial v_i(t,x)}{\partial x} + \eta(x - 1)A(t)v_i(t, x) & 0 < x < 1, \quad t_i < t < t_{i+1}, \\ \text{if } i > 1, \quad v_i(t_i, x) = v_{i-1}(t_i, 1 + SF(x - 1)) \quad \text{if } i = 0, \quad v_0(t, x) = x^{N_0} & 0 < x, y < 1, \\ v_i(t, 0) = p_0(t), \quad v_i(t, 1) = 1 & t_i < t < t_{i+1}. \end{array} \right. \tag{B.2}$$

Following the same procedure, we deduce that $w_i(t, x)$ satisfies the following boundary value problem:

$$\left\{ \begin{array}{ll} \frac{\partial w_i(t,x)}{\partial t} = (d_A + \eta)(1 - x) \frac{\partial w_i(t,x)}{\partial x} & 0 < x < 1, \quad t_i < t < t_{i+1}, \\ w_i(t_i, x) = v_{i-1}(t_i, 1 + \gamma(1 - SF)(x - 1))w_{i-1}(t_i, 1 + SF(x - 1)) & 0 < x, y < 1, \quad i > 1, \\ w_0(t, x) = 1 & 0 < x, y < 1, \quad i = 0, \\ w_i(t, 0) = p_0(t), \quad w_i(t, 1) = 1 & t_i < t < t_i. \end{array} \right. \tag{B.3}$$

We use the method of characteristics to solve both Equation (B.2) and (B.3) for v_i and w_i . Let us assume the initial time is 0 and then we make a change of variables to return to the initial condition at t_i . Equation (B.2) has the characteristic equations:

$$\frac{dX}{dt} = (b_U X - d_U)(1 - X) = (1 - X)(b_U - d_U) - b_U(1 - X)^2, \quad X(0) = x_0, \tag{B.4}$$

$$\frac{dv_i}{dt} = \eta(X - 1)A(t)v_i, \quad v_i(0, x_0) = f(x_0), \tag{B.5}$$

where $f(x) = v_{i-1}(t_i, 1 + SF(x - 1))$ if $i > 1$ and $f(x) = x^{N_0}$ if $i = 0$.

We introduce $Y(t) = \frac{1}{1-X(t)}$ to transform Equation (B.4) into a linear equation for $Y(t)$:

$$\frac{dY}{dt} = (b_U - d_U)Y(t) - b_U, \quad Y(0) = \frac{1}{1 - x_0}.$$

The solution of this equation is

$$Y(t) = e^{(b_U - d_U)t} \left(Y(0) - \frac{b_U}{b_U - d_U} [e^{-(b_U - d_U)t} - 1] \right). \tag{B.6}$$

After some algebra we obtain,

$$x_0 = 1 - \frac{1}{\frac{e^{-(b_U-d_U)t}}{1-x(t)} + b_U \int_0^t e^{-(b_U-d_U)s} ds}. \quad (\text{B.7})$$

The solution of Equation (B.5) is

$$v_i(t, x(t)) = v_i(0, x_0) \exp\left(\eta \int_0^t A(z)(x(z) - 1) dz\right). \quad (\text{B.8})$$

The right hand side contains the term $x(z) - 1$ for intermediate values $x(z)$ with $z \in [0, t)$. To make this expression independent of the characteristic, we notice that (B.7) is valid for $z \in [0, t)$, and for t we have the following equality

$$\begin{aligned} x_0 &= 1 - \frac{1}{\frac{e^{-(b_U-d_U)t}}{1-x(t)} + b_U \int_0^t e^{-(b_U-d_U)s} ds} \\ &= 1 - \frac{1}{\frac{e^{-(b_U-d_U)z}}{1-x(z)} + b_U \int_0^z e^{-(b_U-d_U)s} ds}. \end{aligned} \quad (\text{B.9})$$

Hence

$$x(z) - 1 = -\frac{e^{-(b_U-d_U)t}}{\frac{e^{-(b_U-d_U)t}}{1-x(t)} + b_U \int_z^t e^{-(b_U-d_U)r} dr}. \quad (\text{B.10})$$

Substituting this expression in Equation (B.8), and making the change of variables $t \rightarrow t - t_i$, we obtain an explicit expression for $v_i(t, x)$ for $t \in [t_i, t_{i+1}]$:

$$\begin{aligned} v_i(t, x) &= v_{i-1} \left(t_i, 1 - \frac{B_U SF(1-x)}{(b_U x - d_U) e^{-(b_U-d_U)(t-t_i)} + b_U(1-x)} \right) \\ &\quad \times \exp \left[-B_U \eta (1-x) \int_{t_i}^t \frac{A(s) e^{-B_U(s-t_i)} ds}{b_U(1-x) e^{-B_U(s-t_i)} + (b_U x - d_U) e^{-B_U(t-t_i)}} \right], \end{aligned}$$

where $B_U = b_U - d_U$.

For $i = 0$, $A(t) \equiv 0$ in $[t_0, t_1]$, so the characteristic equation is the same as the one for the TCP without the mean field assumption, therefore,

$$v_0(t, x) = G_0(t, x). \quad (\text{B.11})$$

We now solve for w_i . The characteristic equation of (B.3) is

$$\frac{dX}{dt} = -(d_A + \eta)(1 - X), \quad X(t_0) = x_0, \quad (\text{B.12})$$

from which we obtain

$$x(t) = 1 - [1 - x(t_0)] e^{(d_A + \eta)(t-t_0)}. \quad (\text{B.13})$$

Evaluating at $t = 0$ and making the change of variables $x_0 \rightarrow x, t_0 \rightarrow t$, we obtain

$$x(0) = 1 - (1 - x)e^{-(d_A+\eta)t}. \tag{B.14}$$

Substituting Equation (B.14) in the initial condition of Equation (B.3), we obtain an expression for w_i , namely

$$w_i(t, x) = v_{i-1}(t_i, 1 - \gamma(1 - SF)(1 - x)e^{-(d_A+\eta)(t-t_i)})w_{i-1}(t_i, 1 - SF(1 - x)e^{-(d_A+\eta)(t-t_i)}).$$

Since $p_{n_A}(t) = 0$ for $t \in [t_0, t_1]$, it follows that, for $i = 0$,

$$w_0(t, x) = 1.$$

Appendix C. Function $TCP_{mean}^*(t)$

In this section, we define the function $TCP_{mean}^*(t)$ and prove that $TCP_{mean}^*(t) < TCP_{mean}(t)$.

The function $TCP_{mean}^*(t)$ is defined as follows:

$$TCP_{mean}^*(t) = \hat{v}_i(t, 0)\hat{w}_i(t, 0)$$

such that for $i > 0$,

$$\hat{v}_i(t, x) = \hat{v}_{i-1}(t_i, f_i(t, x))\hat{I}_i(t, x),$$

$$\hat{w}_i(t, x) = \hat{v}_{i-1}(t_i, 1 - \gamma(1 - SF)(1 - x)e^{-(d_A+\eta)(t-t_i)})\hat{w}_{i-1}(t_i, 1 - SF(1 - x)e^{-(d_A+\eta)(t-t_i)}),$$

where n_i is defined in Equation (3.9) and $\hat{I}_i(t, x)$ is defined as

$$\hat{I}_i(t, x) = \exp \left[\frac{-\eta A(t_i^+)(1 - x)}{b_U - d_U} (e^{(b_U-d_U)(t-t_i)} - 1) \right].$$

For $i = 0$, $v_0(t, x) = G_0(t, x)$ and $w_0(t, x) = 1$.

Notice that $TCP_{real}(t)$ and $TCP_{mean}^*(t)$ only differ in the terms $\hat{I}_i(t, x)$ and $I_i(t, x)$, therefore, to prove that $TCP_{real}(t) < TCP_{mean}^*(t)$, it is sufficient to prove that $\hat{I}_i(t, x) < I_i(t, x)$. For this, we notice that

$$\begin{aligned} I_i(t, x) &= \exp \left[-\eta(1 - x)(b_U - d_U) \int_{t_i}^t \frac{A(s)e^{-(b_U-d_U)(s-t_i)} ds}{b_U(1 - x)e^{-(b_U-d_U)(s-t_i)} + (b_Ux - d_U)e^{-(b_U-d_U)(t-t_i)}} \right] \\ &= \exp \left[-\eta \int_{t_i}^t \frac{A(s)e^{-(b_U-d_U)(s-t_i)} ds}{\frac{e^{-(b_U-d_U)(t-t_i)}}{1-x} + \frac{b_U}{b_U+d_U} (e^{-(b_U-d_U)(s-t_i)} - e^{-(b_U-d_U)(t-t_i)})} \right]. \end{aligned}$$

We also note that

$$\begin{aligned}
 & \int_{t_i}^t \frac{A(s)e^{-(b_U-d_U)(s-t_i)} ds}{\frac{e^{-(b_U-d_U)(t-t_i)}}{1-x} + \frac{b_U}{b_U+d_U} (e^{-(b_U-d_U)(s-t_i)} - e^{-(b_U-d_U)(t-t_i)})} \\
 & \leq \int_{t_i}^t \frac{A(s)e^{-(b_U-d_U)(s-t_i)} ds}{\frac{e^{-(b_U-d_U)(t-t_i)}}{1-x}} \\
 & \leq e^{(b_U-d_U)(t-t_i)} (1-x) A(t_i^+) \int_{t_i}^t e^{-(b_U-d_U)(s-t_i)} ds \\
 & = \frac{A(t_i^+)(1-x)}{b_U-d_U} [e^{(b_U-d_U)(t-t_i)} - 1].
 \end{aligned}$$

The first inequality is valid since the term that we eliminated in the denominator is positive. The second inequality is true because $A(t)$ is a decreasing function between the treatment times and at treatment times we have that $A(t_{i+1}^+) < A(t_i^+)$.

Therefore, from the above definition of $\hat{I}_i(t, x)$ it follows that $\hat{I}_i(t, x) < I_i(t, x)$.